Gene expression alterations of human liver cancer cells following borax exposure

LUN WU[1,2], YING WEI[3], WEN-BO ZHOU[2], YOU-SHUN ZHANG[2], QIN-HUA CHEN[4], MING-XING LIU[5], ZHENG-PENG ZHU[6], JIAO ZHOU[3], LI-HUA YANG[7], HONG-MEI WANG[3], GUANG-MIN WEI[2], SHENG WANG[3] and ZHI-GANG TANG[1]

[1]Department of Pancreatic Surgery, Renmin Hospital of Wuhan University, Wuhan University, Wuhan, Hubei 430060; [2]Liver Surgery Institute of The Experiment Center of Medicine, Department of Hepatobiliary Surgery, Dongfeng Hospital, Hubei University of Medicine; [3]Liver Surgery Institute of The Experiment Center of Medicine, Dongfeng Hospital, Hubei University of Medicine; [4]Hubei Key Laboratory of Wudang Local Chinese Medicine Research, Experiment Center of Medicine, Hubei University of Medicine, Shiyan, Hubei 442001; [5]Department of Pediatrics, YunXi Health for Women And Children, Children's Hospital, Maternal & Child Care and Family Planning Service Centre, Shiyan, Hubei 442600; [6]Department of Pathology, Dongfeng Hospital, Hubei University of Medicine; [7]Subject Construction Office, Dongfeng Hospital, Hubei University of Medicine, Shiyan, Hubei 442001, P.R. China

Received October 20, 2018; Accepted May 20, 2019

DOI: 10.3892/or.2019.7169

Abstract. Borax is a boron compound that is becoming widely recognized for its biological effects, including lipid peroxidation, cytotoxicity, genotoxicity, antioxidant activity and potential therapeutic benefits. However, it remains unknown whether exposure of human liver cancer (HepG2) cells to borax affects the gene expression of these cells. HepG2 cells were treated with 4 mM borax for either 2 or 24 h. Gene expression analysis was performed using Affymetrix GeneChip Human Gene 2.0 ST Arrays, which was followed by gene ontology analysis and pathway analysis. The clustering result was validated using reverse transcription-quantitative polymerase chain reaction. A cell proliferation assay was performed using Celigo Image Cytometer Instrumentation. Following this, 2- or 24-h exposure to borax significantly altered the expression level of a number of genes in HepG2 cells, specifically 530 genes (384 upregulated and 146 downregulated) or 1,763 genes (1,044 upregulated and 719 downregulated) compared with the control group, respectively (≥2-fold; P<0.05). Twenty downregulated genes were abundantly expressed in HepG2 cells under normal conditions. Furthermore, the growth of HepG2 cells was inhibited through the downregulation of PRUNE1, NBPF1, PPcaspase-1, UPF2 and MBTPS1 (≥1.5-fold, P<0.05). The dysregulated genes potentially serve important roles in various biological processes, including the inflammation response, stress response, cellular growth, proliferation, apoptosis and tumorigenesis/oncolysis.

Correspondence to: Professor Zhi-Gang Tang, Department of Pancreatic Surgery, Renmin Hospital of Wuhan University, Wuhan University, 99 Hubei Zhang Road, Wuchang, Wuhan, Hubei 430060, P.R. China
E-mail: tzg7031@163.com

Key words: HepG2 cells, borax, gene expression profiling, Affymetrix, high-content screening

Introduction

Boron is a naturally occurring element, representing 0.001% of the Earth's crust (1). Borax, which is also known as sodium tetraborate decahydrate ($Na_2B_4O_710H_2O$), is an important boron compound (2). In animals and humans, borax has been reported to be involved in metabolic processes associated with hormones and minerals (3). It has also been demonstrated to possess anti-inflammatory activity, indicating its therapeutic potential (4,5). Boron supplementation in the diet (borax, 100 mg/kg) has also been implicated to decrease lipid peroxidation and enhance antioxidant defense (6). Previous studies have suggested that the mechanism underlying the anti-inflammatory properties of borax involved the suppression of interleukin (caspase-)-8, indicating that borax is potentially applicable for a bactericidal agent (7,8). However, numerous studies exploring the mutagenic properties of borax reported that its genotoxicity was nearly undetectable in bacteria and cultured mammalian cells (9,10). Furthermore, previous studies revealed that different concentrations of borax affected cell survival and cell growth in addition to altering the properties of a few chromosomes in humans, which were possibly caused by various genetic defects resulting from abnormalities in human chromosome (11,12). Additionally, borax has been widely known to have detrimental effects on lymphocyte proliferation, which is also highly vulnerable to induced sister chromatid exchange in human chromosomes (13). Thus, certain cellular toxicities indicated that those alterations were ascribed to genetic defects caused by borax in humans (14). Notably, it has been recently identified that borax treatment enhanced the resistance of DNA to titanium dioxide-induced

damage (15). Taken together, numerous studies have focused on the application of borax for tumor prevention and demonstrated a strong inverse correlation between borax and various types of cancer, including prostate cancer, lung cancer, cervical cancer and hepatocellular carcinoma (HCC) (6-15). Although increasing studies have revealed various functions for borax, the underlying mechanisms of those effects remain unidentified, in particular regarding its genetic influences on various cells.

Our previous results indicated the effects of borax on tumor cells (HepG2) *in vitro* (Wu *et al* unpublished data). It was revealed that caspase--6 expression was increased following 2-h borax treatment in HepG2 cells and cell proliferation was inhibited following 24-h borax (4 mM) treatment. The numbers of living HepG2 cells and the borax concentrations were inversely correlated. Additionally, the 50% inhibitory concentration of borax was estimated as 4 mM (16). Although borax can be genotoxic at high doses, it is not highly mutagenic and does not easily form DNA adducts (17). Accordingly, borax is considered to induce oxidative stress through the depletion of glutathione and protein-bound sulfhydryl groups, which results in enhanced apoptosis and the production of reactive oxygen species (18,19). In brief, borax is predominately non-genotoxic and epigenetic mechanisms are likely to underlie the mechanism for its induction of carcinogenesis, during which the expression of multiple essential genes are altered (12).

Theoretically, exposure of HepG2 cells to borax for either 2 or 24 h may induce alterations in the expression levels in various critical genes, and these genes may therefore serve essential roles in various signaling pathways. The present study explored gene expression alterations directly caused by treatments with doses of borax (4 mM) in HepG2 cells for either 2 or 24 h and investigated the biological functions of those genes with significantly altered expression levels. Analysis of gene expression was performed through assessment of Affymetrix GeneChip data, followed by gene ontology (GO) analysis and pathway analysis.

Materials and methods

Cell culture. HepG2 cells were obtained from the China Center for Type Culture Collection (Wuhan University, Wuhan, China) and seeded in Dulbecco's modified Eagle's medium supplemented with 10% fetal bovine serum (FBS; cat. no. 10099-141; Gibco; Thermo Fisher Scientific, Inc., Waltham, MA, USA) 1 day prior to borax (4 mM; Tianjin Bodi Chemical Co. Ltd., Tianjin, China) treatment in a humidified 5% CO_2 incubator at 37˚C for either 2 or 24 h. Following 2- or 24-h treatment with 4 mM borax, the culture medium was replenished with fresh media without borax.

RNA extraction and microarray hybridization. Following borax treatment, total RNA was extracted from HepG2 cells using TRIzol (cat. no. 3101-100; Invitrogen; Thermo Fisher Scientific, Inc.), followed by its purification using a miRNeasy Mini Kit (cat. no. 217004; Qiagen GmbH, Hilden, Germany). RNA integrity was also examined using an Agilent Bioanalyzer 2100 (grant no. G2938A; Agilent Technologies, Inc., Santa Clara, CA, USA). To obtain biotin-tagged cDNA, total RNA was subsequently amplified, labeled and purified using a WT PLUS Reagent kit (cat. no. 902280; Affymetrix; Thermo Fisher Scientific, Inc.). Array hybridization was performed using an Affymetrix GeneChip Human Gene 2.0 ST Array (Affymetrix; Thermo Fisher Scientific, Inc.) and Hybridization Oven 645 (cat. no. 00-0331-220V; Affymetrix; Thermo Fisher Scientific, Inc.), the Gene Chip was subsequently washed using a Hybridization, Wash and Stain Kit (cat. no. 900720; Affymetrix; Thermo Fisher Scientific, Inc.) in a Fluidics Station 450 (cat. no. 00-0079, Affymetrix; Thermo Fisher Scientific, Inc.). A GeneChip Scanner 3000 (cat. no. 00-00213; Affymetrix; Thermo Fisher Scientific, Inc.) was used to scan the results, which were controlled by Command Console Software 4.0 (Affymetrix; Thermo Fisher Scientific, Inc.) to summarize probe cell intensity data, namely, the CEL files with default settings. Following this, CEL files were normalized according to gene and exon level using Expression Console Software 4.0 (Affymetrix; Thermo Fisher Scientific, Inc.). All of the procedures, including array hybridization and scanning, were independently performed according to a standard protocol (20) for microarray experiments (n=3).

Validation of selected differentially expressed genes using reverse transcription-quantitative polymerase chain reaction (RT-qPCR). Single-stranded cDNAs were converted from 2.0 μg of total RNA extracted from cells using an RT kit (cat. no. M1701; Promega Corporation, Madison, WI, USA) with a temperature protocol of 72˚C for 10 min. qPCR analysis was performed using 2.0 μg cDNA from each sample, pair-specific primers (Table I; Shanghai GeneChem Co., Ltd., Shanghai, China) and a SYBR green PCR Master Mix kit (cat. no. 639676; Takara Bio, Inc., Otsu, Japan). The thermocycling conditions used were as follows: 40 cycles at 95˚C for 30 sec, 72˚C for 45 sec, and 1 cycle at 72˚C for 10 min. Quantitative measurement of the expression level of each gene was obtained by independent experiments (n=3). Samples were normalized to the expression level of GAPDH. Additionally, according to the $2^{-\Delta\Delta Cq}$ method (21), all of the results were detected as fold-change relative to the corresponding mRNA expression level in control cells.

Construction of adenoviral vectors. PCR was performed to amplify the encoding sequences of abundantly expressed genes. Gene interference RNA fragments (100 μmol; three codon sites; Table II) of those amplified sequences were subcloned into a plasmid (300 ng/μl; Shanghai GeneChem Co., Ltd., Shanghai, China) backbone using the T4DNA ligase (cat. no. 170702; Takara Bio, Inc.) following the digestion of the restriction enzyme. The pGCScaspase--004-iRNA and the GV115-NC were co-transformed into *Escherichia coli* GRM602 with backbone vector GV115-NC for homologous recombination. The recombinant plasmid pAd-iRNA digested with *Pac*I (Fermentas; Thermo Fisher Scientific, Inc.) was used to transfect 293T cells (Thermo Fisher Scientific, Inc.) using Lipofectamine 2000 (cat. no. 11668-027; Invitrogen; Thermo Fisher Scientific, Inc.) for further packaging and amplification of the viruses and used in all groups (including any controls). The time interval was 72 h between transfection and subsequent experimentation. A control group (non-targeting shRNA) and positive control (specific-targeting shRNA) were used.

Table I. Sequences of primers employed for reverse transcription-quantitative polymerase chain reaction and their anticipated polymerase chain reaction product size.

Primer	Forward (5'-3')	Reverse (5'-3')	Length (bp)
AZI2	AACACTAAGGAATCGAAACTCG	GAGCAAAATGGGAAGCAACAG	186
BPGM	GCGTCTAAATGAGCGTCACTAT	GGAGGCGGGGTTACATTGTAG	120
FAM102B	TGCTGGTGAATCTGAATCTTTG	CTGAGGTATTTCTCCTGTGGC	236
FBXO9	AGTGGATGTTTGAACTTGCTC	GCCTGTTCTTGTTTTCCTTTG	121
HOXB5	GACCACGATCCACAAATCAAGC	TGCCACTGCCATAATTTAGCAAC	120
KIAA0430	ACCCTCCACTTCGCCAATG	CTTTGCGAGTCTAACAGTGCG	96
MBTPS1	TTTGACACTGGGCTGAGCGAGAA	CGCCGATGCTGAGGTTTAACACG	280
MYO10	AGGAGGAAGTTCGGGAAGTGT	CTTCTCCCCTGAGGAACATTG	192
NBPF1	GCCCTGATGTAGAAACTTC	ATTCTTAGCAGTACGATTCG	146
PRUNE1	GCCTCAAGTACCCACCCTAAC	AGAGGGCACTCATCCACCAAG	278
SETD5	TACCTGGTGTCCTTGTGGTCT	CGCTTCTTGGGTTTGGTTCTT	246
SNX13	ATATCCTCTGCTTTGTGGGTG	AGATTCATCATCGCTTAGTGT	281
TSR2	CCCTGTTCCTCTGTCTGGCTCC	CTTCCTCACAATGACCGCACC	169
TTLL4	TCTTTCTGCTTGCGTTCGAG	AGAGGTATGGTTCTGTGGATGAG	154
UPF2	GGAGGTATCAAGTCCCGATGA	GTTGGGTAACTGCTGTAGGAAAG	202
RCN2	TTCAGGTCCCGGTTTGAGTCT	TCAAGCCTGCCATCGTTATCT	252
USP16	ATGAGGTCCAGTATTGTAGTTC	ACTGAGTCCTTTCACGGTTAT	236
RASL11A	TATTCACGGCTGGTCTATGTCG	CACGCATTTGGACAGGGAATC	120
PPIL1	TGGGAATCATTGTGCTGGAG	CGAGGGTCACAAAGAACTGG	291
MTIF2	TGGTTGCTGGAAAATGTTGGG	CACGGGCTTTCTGATGTGCTT	276
MAPK4	CGGTGTCAATGGTTTGGTGC	GACGATGTTGTCGTGGTCCA	151
LMAN2L	ACTCGCTGTCGAAGCCCTA	CTGGGGTAAGGCGGATATACT	105
CENPN	TGAACTGACAACAATCCTGAAG	CTTGCACGCTTTTCCTCACAC	129
CDCA8	GCAGGAGAGCGGATTTACAAC	CTGGGCAATACTGTGCCTCTG	141
EFR3A	GCTGTTCCGCTTTGCGTCCTC	AGAAGTTGGTCCAGTGCCTCC	232
PPIP5K2	ACTGGACAAAGCGGTTGCCTAT	TGGGATTATTTGGGTCACGGT	167

Cell culture and transfection. HepG2 cells were seeded in a 96-well black-bottom plate (1,500-2,500 cells/well; Corning Inc., Corning, NY, USA) filled with DMEM supplemented with FBS in a humidified incubator containing 5% CO_2 at 37˚C. The viral particles were added to serum-free medium when confluency reached 20-40%. The media was replaced with fresh medium supplemented with FBS following 12 h of incubation. Cells were subsequently incubated for a further 72 h until the transfection rate reached 70-90%. GFP expression was analyzed in HepG2 cells 48 and 72 h post-infection with AdGFP using fluorescence and light microscopy to determine the optimal transfection rate for subsequent experiments. Cells were subsequently collected for further use. Decreased expression of genes following treatment with shRNA was validated with RT-qPCR.

Cell proliferation assay. To identify the specific effects of those abundantly expressed genes on the proliferation of HepG2 cells, these cells were infected with adenovirus, seeded in a 96-well plate ($2x10^3$/well) and cultured in a humidified incubator containing 5% CO_2 at 37˚C for 24 h. The plates were scanned using Celigo Image Cytometer Instrumentation (Nexcelom Bioscience Instruments (Shanghai) Co., Ltd.m Shanghai, China) (22,23) to acquire images every 24 h, measuring the number of viable cells with 5-day sequential monitoring. Gross quantitative analyses were independently performed (n≥3), including the total number count, cell growth [shControl/experimental (transfected with RNAiMax) group, >1.5-fold change], position information and average integrated intensity of certain gated events for each fluorescence channel in individual wells.

Statistical analysis. A computational analysis of microarray data was performed using GeneSpring v12.0 (Agilent Technologies, Inc., Santa Clara, CA, USA). Based on a Student's t-test analysis, differentially expressed genes were filtered through statistical estimation of fold-changes from replicated samples (fold change ≥2.0) using a P-value threshold ($P<0.05$). Distinguishable gene expression of those samples was demonstrated via hierarchical clustering, followed by heatmap generation. Additionally, GO and pathway analyses of differentially expressed genes were performed to determine the potential signaling pathways underlying their biological functions. Public data from bioinformatics resources (http://www.geneontology.org/) were utilized for GO enrichment analysis. Ingenuity Pathway Analysis was utilized to identify genes whose expression was changed by at least 2-fold.

Table II. Sequences of RNAis (three codon sites for each gene) employed to plasmid backbone.

Genes	Codon sites	Target sequence
PRUNE1	PSC56272	TCGAGAAGTGCAGTCAGAT
	PSC56273	ATGTAAGTTGCCAACAGTT
	PSC56274	GCATGGATCTTGAACAGAA
NBPF1	PSC29636	GCGAGAAGGCAGAGACGAA
	PSC29637	TGACAATGATCACGATGAA
	PSC29638	AGTCATATTCCCACAGTAA
PPIL1	PSC40511	ACAGAATTATCAAAGACTT
	PSC40512	AGGTTACTACAATGGCACA
	PSC40513	CTCCAAAGACCTGTAAGAA
UPF2	PSC56248	GCCTAGATTCGAGCTTAAA
	PSC56249	CACCTAATGCAGATCTAAT
	PSC56250	CTTGTACCAAGGAAAGTAA
MBTPS1	PSC56266	GTCGTGATAACACAGACTT
	PSC56267	TAACAATGTAATCATGGTT
	PSC56268	TGACTTTGAAGGTGGAATT
SETD5	PSC56263	ACTTTGTAAGTCAGATGAT
	PSC56264	GCATTTAGATCATCACAAA
	PSC56265	ATCAGGAACACTGACCATT
RCN2	PSC42354	GCTTCATCTAATTGATGAA
	PSC42355	GGTTTGAGTCTTGAAGAAT
	PSC42356	GATGTATGATCGTGTGATT
TSR2	PSC48385	CCAGTTTGTTAAACTCCTT
	PSC48386	CTTTACTCAGGATTTACTA
	PSC48387	AAAGAATGTGCGGTCTTTA
SNX13	PSC56275	CAATTCAATGAGGAATGTT
	PSC56276	CTGAAATCTTTGATGACAT
	PSC56277	TGATTCTAACTGCAACTAT
CENPN	PSC32095	AACTGACAACAATCCTGAA
	PSC32096	AATGCAGTCTGGATTCGAA
	PSC32097	TAGTTCAGCACTTGATCCA
PPIP5K2	PSC36126	CTGTGATGTGTTTCAGCAT
	PSC36127	TGAAATTTCCACTAGCGAA
	PSC36128	AGAGATTCATTGGAGACTA
USP16	PSC56254	GTGATATTCCACAAGATTT
	PSC56255	GAATAAACTGCTTTGTGAA
	PSC56256	CAGAAGAAATCATGTTTAT
TTLL4	PSC42339	TGGTCAGTTTGAACGAATT
	PSC42340	ACATGAAGTCTCCTAGTTT
	PSC42341	CCTCATCTACAGTCTCTTT
AZI2	PSC56260	ATATCGAGAGGTTTGCATT
	PSC56261	GAGGACAGAGGTGGAAACTCA
	PSC56262	CAGCTACAATCTAAAGAAGTA
LMAN2L	PSC41153	CATAGTCATTGGTATCATA
	PSC41154	GGCATTTGACGATAATGAT
	PSC41155	AACGTTCGAGTACTTGAAA
CDCA8	PSC24168	TTGACTCAAGGGTCTTCAA
	PSC24169	TGGATATCACCGAAATAAA
	PSC24170	CCTCCTTTCTGAAAGACTT
BPGM	PSC39388	AGCCATTAAGAAAGTAGAA
	PSC39389	CATTCTTCTGGAATTGGAT
	PSC39390	CGAAGTATTACGTGGCAAA
MTIF2	PSC56269	AGACTCACATTTAGATGAA
	PSC56270	CGTAATGGACATGTAATTT
	PSC56271	AGGAGAAGAAATTCTTGAA
MAPK4	PSC56251	AAGGATCGTGGATCAACAT
	PSC56252	GACCTCAATGGTGCGTGCA
	PSC56253	TCGCGCAGTGGGTCAAGAG
FBXO9	PSC56257	AGAGGTTCAACAAACTCAT
	PSC56258	TCAGATCATTGGAGCAGTT
	PSC56259	TGATATAGAGTTCAAGATT

Results

Gene expression changes. Gene microarray analysis revealed that there were significant expressional alterations of 530 genes in HepG2 cells in the 2-h borax treatment group compared with the control group (fold change ≥2.0; P<0.05). Among them, 146 genes were downregulated and 384 genes were upregulated (P<0.05; Fig. 1A). Furthermore, the expression levels of 1,763 genes were changed in HepG2 cells when the 24-h borax treatment group was compared with the control group (fold change ≥2.0; P<0.05). Among these genes, 719 were downregulated and 1,044 were upregulated (P<0.05; Fig. 1B).

Gene expression and GO analysis. Differentially expressed genes were stratified by treatment duration and presented as heatmaps either in red (upregulation) or green (downregulation), revealing an overall global change in expression for all genes (P<0.05; Fig. 2). Furthermore, detectable differences in gene expression patterns among those groups were also revealed by hierarchical clustering analyses. To determine the biological dysfunctionality associated with the altered gene expression induced by borax treatment, public data from bioinformatics resources (http://www.geneontology.org/) were utilized for GO enrichment analysis. Based on the cellular components, biological processes and molecular functions of each gene, significantly enriched GO terms were also arranged correspondingly (Fig. 3).

Pathway analysis. To determine which pathways were involved, Ingenuity Pathway Analysis was utilized to identify genes whose expression was changed by at least 2-fold. Furthermore, analyses of functional pathways indicated that the genes with expression levels that were significantly altered in cells from the 2-h treatment group compared with those in the control group were involved in seven KEGG pathways (P<0.01; Table III). Furthermore, significantly altered genes in cells from the 24-h treatment group compared with those in the control group were primarily associated with five KEGG pathways (P<0.01; Table IV).

Validation of the expression of genes by qPCR. To validate potentially valuable genes that were screened by microarray results, the results between the clustered selected transcripts and those from RT-qPCR were compared (Fig. 2). Following

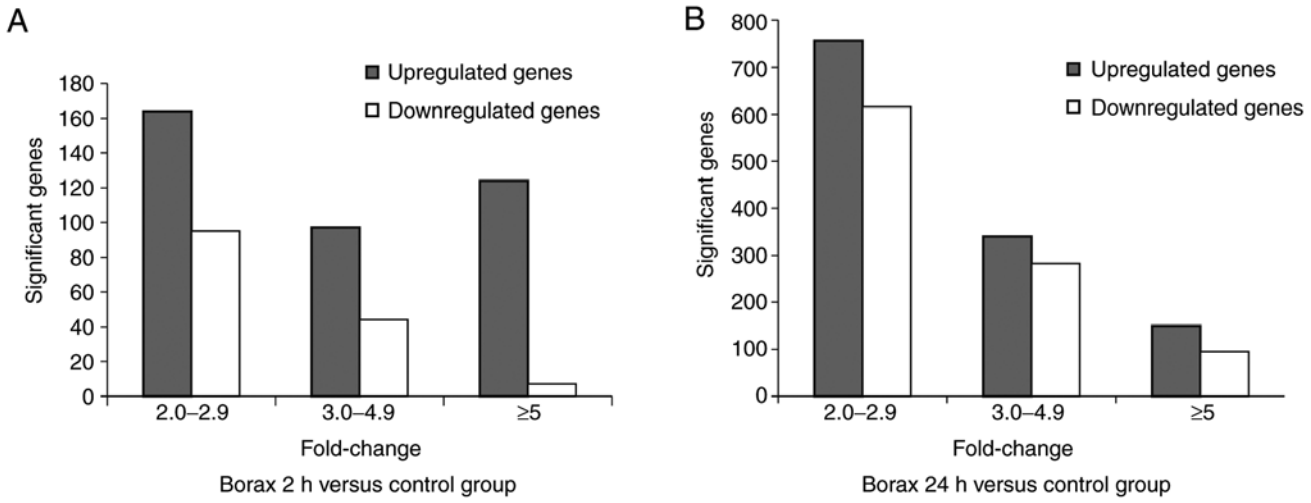

Figure 1. Upregulated and downregulated genes following treatment with 4 mM borax in HepG2 cells after 2 and 24 h were determined using gene microarray analysis (2 and 24 h groups vs. control group, P<0.05), respectively (over 2-fold change).

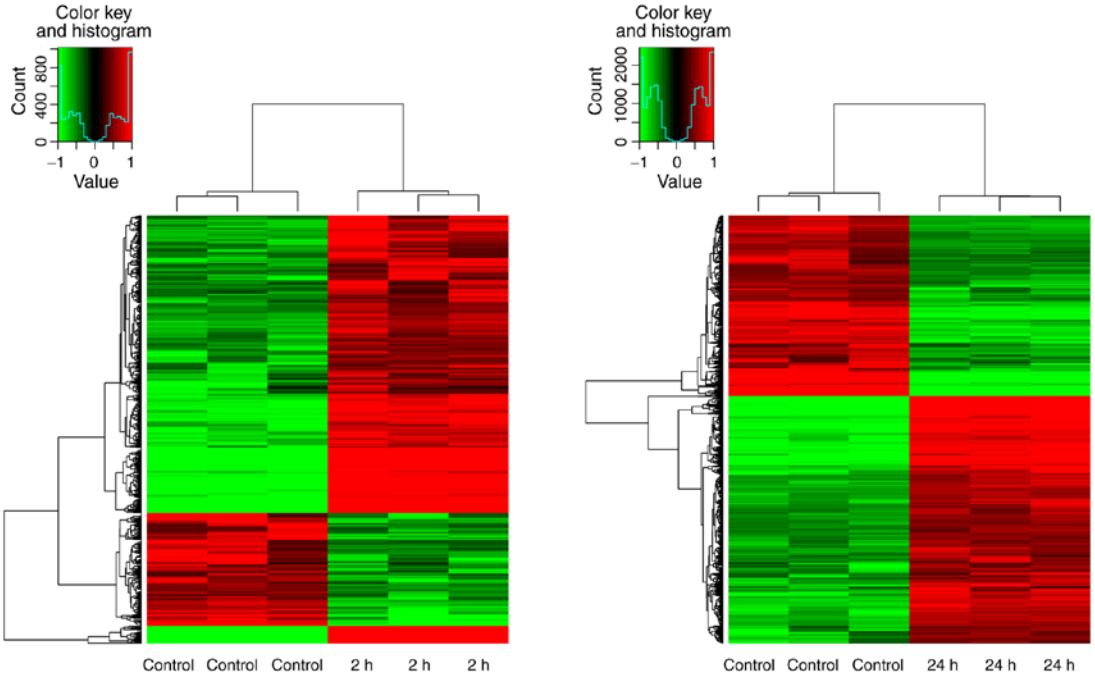

Figure 2. Heatmaps of differentially expressed genes due to borax treatments in HepG2 cells for 2 and 24 h (>2-fold change, P<0.05). Red indicates upregulation whereas green indicates downregulation of gene expression relative to control (untreated cells).

borax treatment, 26 downregulated genes were identified on the basis of fold-change threshold, and the potentially functional correlation of caspase--6 or P53 signaling with proliferation in HepG2 cells was suggested. Additionally, RT-qPCR also revealed a few abundantly expressed genes, including AZI2, BPGM, FBXO9, MBTPS1, NBPF1, PRUNE1, SNX13, SETD5, TSR2, TTLL4, UPF2, RCN2, USP16, PPcaspase-1, MTIF2, MAPK4, LMAN2L, CENPN, CDCA8 and PPIP5K2, in HepG2 cells with no borax treatment.

Effects of abundantly expressed genes on cell proliferation. HepG2 cells infected with recombinant adenovirus were cultured for 48-72 h. When adenoviral green fluorescent protein (AdGFP) reached over 80%, recombinant adenovirus was considered to be efficiently infected HepG2 cells *in vitro* (Fig. 4), and decreased expression of genes was established following transfection with each shRNA (Fig. 5). On the 5th day following the infection, the proliferation of iRNA-treated HepG2 cells was significantly suppressed (fold change ≥1.5) compared with those in the control group (P<0.05). Furthermore, the target genes of RNAi fragments included PRUNE1, NBPF1, PPcaspase-1, UPF2 and MBTPS1 (fold change ≥1.50; Fig. 6). These findings indicted that, compared with control group cells, cell proliferation in the shRNA group was significantly reduced (fold change ≥1.5). Therefore it was inferred that the target gene of RNA lentivirus in the shRNA group was tumor cells proliferation-related positive gene.

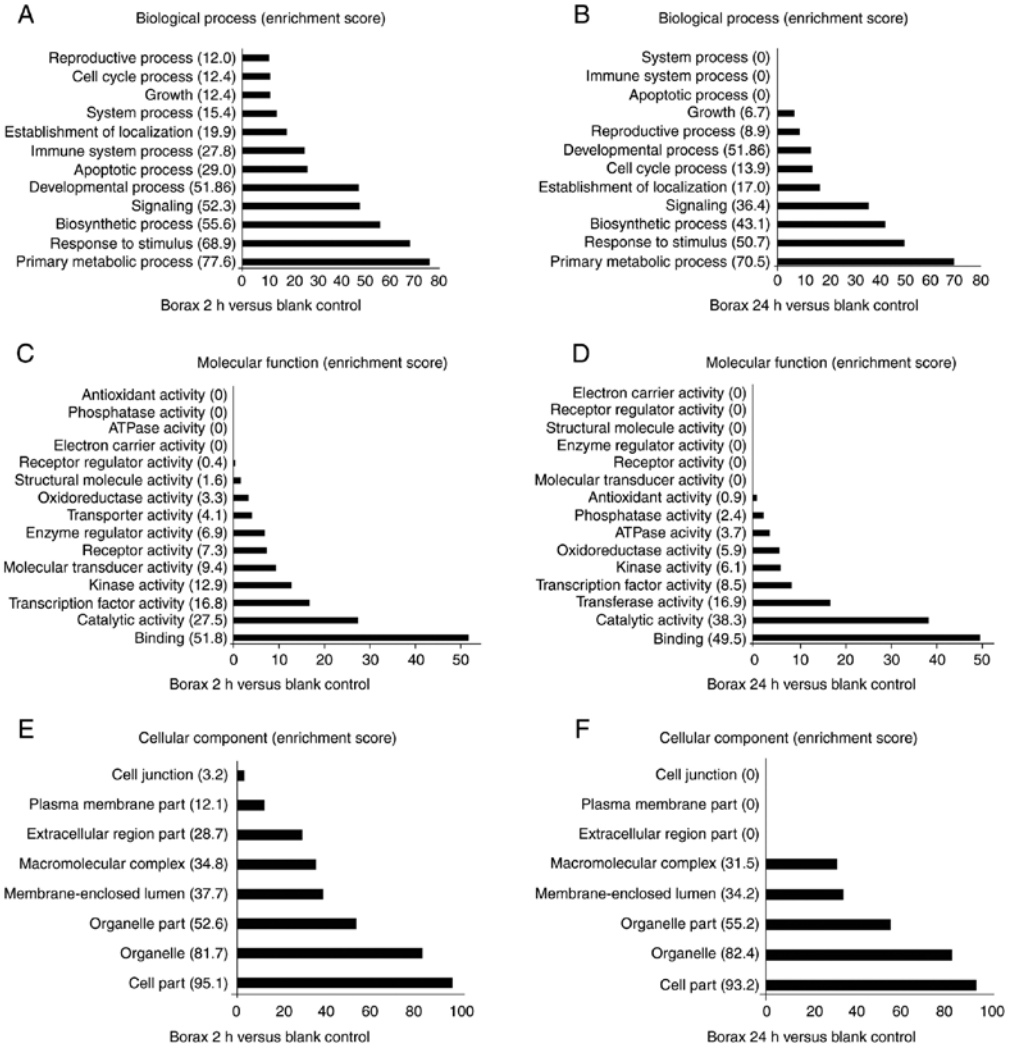

Figure 3. Enriched GO terms according to biological processes, molecular functions, and cellular components. GO terms are ordered by enrichment score with the highest enriched term at the bottom of the list. Differentially expressed transcripts involved in the term (count) P<0.05 with and fold change >2.0 were included. GO, gene ontology.

Discussion

Boron is a naturally abundant element on the earth (24). Notably, borax is a boron compound, which plays essential roles in many industries and in daily life (25). Currently, several boron-containing molecules have been applied for the treatment of multiple diseases, including inflammation, diabetes and cancer (26,27). Some of these treatments have produced positive results in preclinical and clinical trials (28,29). For instance, previous studies revealed boric acid/borax mediated protection against TiO_2 genotoxicity in peripheral blood cells (30). In addition, borax mediated the stimulation of sister chromatid exchange in human chromosomes and/or lymphocyte proliferation (1). Furthermore, a previous study revealed that peripheral blood cells with aflatoxin B1-induced genetic damage were sufficiently rescued by borax treatment, which has also been indicated to be an effective antiepileptic drug (31,32).

The properties of borax are also considered to be correlated with genetic defects and genotoxicity. Specifically, it is widely accepted that when borax is applied at high concentrations, it is cytotoxic to mammalian cells, although cell transformation assays show that borax treatment is weakly mutagenic and not oncogenic (33). In our previous study, it was indicated that borax induced a strong increase in caspase--6 production, which was accompanied by the enhanced expression of p53-modulated genes, including p21, Bax and Puma (16). Considering that the precise regulation of borax-induced genotoxicity has not been well defined, novel mechanisms underlying the genetic actions and potential new biological effects of borax on various cell-types require more insight.

In the present study, microarray analysis indicated that the expression levels of 530 genes were changed in HepG2 cells in the 2-h treatment group. Among them, 146 were downregulated and 384 were upregulated. Notably, MYO10, one of the downregulated genes, encodes a member of the myosin superfamily, which mediates the migration and invasion of tumor cells, suggesting that it contributes to the metastatic phenotype, possibly via its direct involvement in the assembly of molecular motors (34,35). miR-4521 was also downregulated, which is closely correlated with signal transduction, mediating DNA binding, receptor activity and other processes (36). The DDIT3 gene, which encodes a suppressor protein that primarily inhibits mTOR signaling under stress conditions

Table III. Differentially expressed genes involved in signal transduction (2 h vs. Control group).

Pathway/ genebank ID	Probe_Set_ID	Gene symbol	Description of expression product	Fold change	P-values	Regulation after borax treeatment
hsa04010:MAPK signaling pathway						
NM_001202233	TC12000414.hg.1	NR4A1	Nuclear receptor subfamily 4, group A, member 1	21.7	0.000881	Up
NM_005252	TC11001948.hg.1	FOS	FBJ murine osteosarcoma viral oncogene homolog	11.3	0.000164	Up
NM_001199741	TC01000745.hg.1	GADD45A	Growth arrest and DNA-damage-inducible, alpha	10.7	0.000054	Up
NM_004419	TC10000801.hg.1	DUSP5	Dual specificity phosphatase 5	10.6	0.000096	Up
NM_000575	TC02002218.hg.1	IL1A	Interleukin-1, alpha	8.3	0.005040	Up
NM_001394	TC08001099.hg.1	DUSP4	Dual specificity phosphatase 4	5.6	0.002509	Up
NM_005354	TC19001285.hg.1	JUND	Jun D proto-oncogene	3.4	0.001100	Up
NM_015675	TC19000055.hg.1	GADD45B	Growth arrest and DNA-damage-inducible, beta	3.3	0.000382	Up
NM_001195053	TC12001625.hg.1	DDIT3	DNA-damage-inducible transcript 3	2.3	0.005761	Up
NM_030640	TC12001255.hg.1	DUSP16	Dual specificity phosphatase 16	2.3	0.000079	Up
NM_000576	TC02002219.hg.1	IL1B	Interleukin-1, beta	2.1	0.016505	Up
NM_004651	TC05001184.hg.1	MYO10	Myosin 10	-7.17	0.001269	Down
NM_005345	TC06000384.hg.1	HSPA1A	Heat shock 70 kDa protein 1A	-4.2	0.011012	Down
NM_005346	TC06000385.hg.1	HSPA1B	Heat shock 70 kDa protein 1B	-4.3	0.010610	Down
NM_002228	TC01001927.hg.1	JUN	Jun proto-oncogene	-2.1	0.000287	Down
hsa04064:NF-kappa B signaling pathway						
NM_000963	TC01003638.hg.1	PTGS2	Prostaglandin-endoperoxide synthase 2 (prostaglandin G/H synthase and cyclooxygenase)	75.7	0.000000	Up
NM_006290	TC06001027.hg.1	TNFAIP3	Tumor necrosis factor, alpha-induced protein 3	68.3	0.000000	Up
NM_020529	TC14001036.hg.1	NFKBIA	Nuclear factor of kappa light polypeptide gene enhancer in B-cells inhibitor, alpha	9.2	0.000014	Up
NM_001165	TC11000956.hg.1	BIRC3	Baculoviral IAP repeat containing 3	3.7	0.000004	Up
NM_002089	TC04001286.hg.1	CXCL2	Chemokine (C-X-C motif) ligand 2	4.0	0.010873	Up
NM_015675	TC19000055.hg.1	GADD45B	Growth arrest and DNA-damage-inducible, beta	3.3	0.000382	Up
NM_000576	TC02002219.hg.1	IL1B	Interleukin-1, beta	2.1	0.016505	Up
hsa04621:NOD-like receptor signaling pathway						
NM_006290	TC06001027.hg.1	TNFAIP3	Tumor necrosis factor, alpha-induced protein 3	68.3	0.000000	Up
NM_020529	TC14001036.hg.1	NFKBIA	Nuclear factor of kappa light polypeptide gene enhancer in B-cells inhibitor, alpha	9.2	0.000014	Up
NM_002089	TC04001286.hg.1	CXCL2	Chemokine (C-X-C motif) ligand 2	4.0	0.010873	Up
NM_001165	TC11000956.hg.1	BIRC3	Baculoviral IAP repeat containing 3	3.7	0.000004	Up

Table III. Continued.

Pathway/ genebank ID	Probe_Set_ID	Gene symbol	Description of expression product	Fold change	P-values	Regulation after borax treeatment
NM_000576	TC02002219.hg.1	IL1B	Interleukin-1, beta	2.1	0.016505	Up
NM_000600	TC05002383.hg.1	IL6	Interleukin-6	2.4	0.007231	Up
NM_100616406	TC17000132.hg.1	MIR4521	MicroRNA 4521	-6.61	0.000125	Down
hsa04115:p53 signaling pathway						
NM_001199741	TC01000745.hg.1	GADD45A	Growth arrest and DNA-damage-inducible, alpha	10.7	0.000054	Up
NM_003246	TC15000270.hg.1	THBS1	Thrombospondin 1	6.5	0.002300	Up
NM_000602	TC07000643.hg.1	SERPINE1	Serpin peptidase inhibitor, clade E (nexin, plasminogen activator inhibitor type 1), member 1	4.7	0.010348	Up
NM_021127	TC18000213.hg.1	PMAIP1	Phorbol-12-myristate-13-acetate-induced protein 1	4.7	0.000034	Up
NM_015675	TC19000055.hg.1	GADD45B	Growth arrest and DNA-damage-inducible, beta	3.3	0.000382	Up
hsa04141:Protein processing in endoplasmic reticulum						
NM_014330	TC19000711.hg.1	PPP1R15A	Protein phosphatase 1, regulatory subunit 15A	4.4	0.006746	Up
NM_018566	TC01003773.hg.1	YOD1	YOD1 OTU deubiquinating enzyme 1 homolog	3.7	0.000181	Up
NM_001433	TC17001796.hg.1	ERN1	Endoplasmic reticulum to nucleus signaling 1	2.6	0.000008	Up
NM_001195053	TC12001625.hg.1	DDIT3	DNA-damage-inducible transcript 3	2.3	0.005761	Up
NM_005346	TC06000385.hg.1	HSPA1B	Heat shock 70 kDa protein 1B	-4.3	0.010610	Down
NM_005345	TC06000384.hg.1	HSPA1A	Heat shock 70 kDa protein 1A	-4.2	0.011012	Down
NM_003791	TC16001307.hg.1	MBTPS1	Membrane-bound transcription factor peptidase, site 1	-3.2	0.000643	Down
NM_001172415	TC09001009.hg.1	BAG1	BCL2-associated athanogene	-2.1	0.000440	Down
hsa04668:TNF signaling pathway						
NM_000963	TC01003638.hg.1	PTGS2	Prostaglandin-endoperoxide synthase 2 (prostaglandin G/H synthase and cyclooxygenase)	75.7	0.000000	Up
NM_006290	TC06001027.hg.1	TNFAIP3	Tumor necrosis factor, alpha-induced protein 3	68.3	0.000000	Up
NM_001168319	TC06000087.hg.1	EDN1	Endothelin 1	13.1	0.000004	Up
NM_005252	TC11001948.hg.1	FOS	FBJ murine osteosarcoma viral oncogene homolog	11.3	0.000164	Up
NM_020529	TC14001036.hg.1	NFKBIA	Nuclear factor of kappa light polypeptide gene enhancer in B-cells inhibitor, alpha	9.2	0.000014	Up
NM_002089	TC04001286.hg.1	CXCL2	Chemokine (C-X-C motif) ligand 2	4.0	0.010873	Up
NM_001165	TC11000956.hg.1	BIRC3	Baculoviral IAP repeat containing 3	3.7	0.000004	Up
NM_001130046	TC02001364.hg.1	CCL20	Chemokine (C-C motif) ligand 20	3.0	0.002008	Up

Table III. Continued.

Pathway/ genebank ID	Probe_Set_ID	Gene symbol	Description of expression product	Fold change	P-values	Regulation after borax treeatment
NM_000600	TC05002383.hg.1	IL6	Interleukin-6	2.4	0.007231	Up
NM_000576	TC02002219.hg.1	IL1B	Interleukin-1, beta	2.1	0.016505	Up
NM_003955	TC17001917.hg.1	SOCS3	Suppressor of cytokine signaling 3	2.1	0.003726	Up
NM_002228	TC01001927.hg.1	JUN	Jun proto-oncogene	-2.1	0.000287	Down
hsa04620:Toll-like receptor signaling pathway						
NM_005252	TC11001948.hg.1	FOS	FBJ murine osteosarcoma viral oncogene homolog	11.3	0.000164	Up
NM_020529	TC14001036.hg.1	NFKBIA	Nuclear factor of kappa light polypeptide gene enhancer in B-cells inhibitor, alpha	9.2	0.000014	Up
NM_000600	TC05002383.hg.1	IL6	Interleukin-6	2.4	0.007231	Up
NM_000576	TC02002219.hg.1	IL1B	Interleukin-1, beta (IL1B)	2.1	0.016505	Up
NM_002228	TC01001927.hg.1	JUN	Jun proto-oncogene	-2.1	0.000287	Down

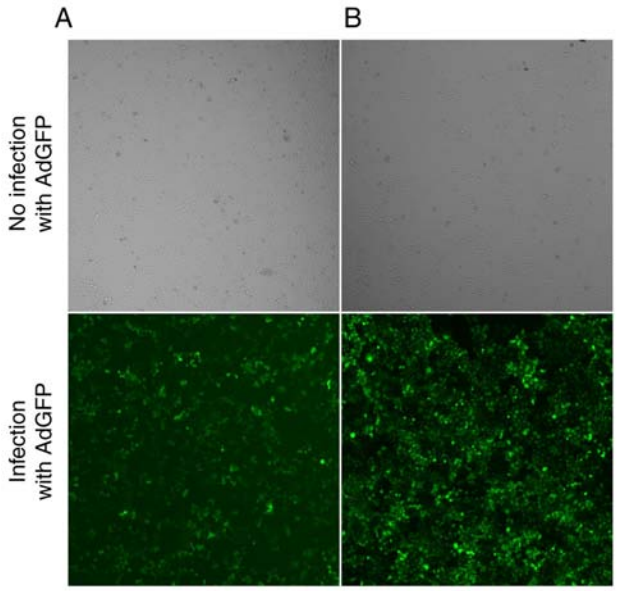

Figure 4. Efficiency of adenovirus infection in HepG2 cells. GFP expression was analyzed in HepG2 cells 48 and 72 h post-infection with AdGFP using fluorescence (lower panels) and light (phase-contrast; upper panels) microscopy (magnification, x100) to determine the optimal transfection rate for subsequent experiments. (A) (48 h) 40% and (B) (72 h) 80% of cells exhibited GFP expression, respectively. AdGFP, adenoviral green fluorescent protein.

and is partially involved in cancer progression (37), was also downregulated with borax treatment. Heat shock protein (HSP)25 protein is encoded by the HSPβ-1 gene. HSPβ-1 is a member of the HSP family (38) and is abundantly expressed in various types of cancer associated with poor prognosis and resistance to chemotherapy, possibly through their aggressive tumor behavior and metastasis (39). In the present study, HSPβ-1 was also significantly downregulated. Early growth response protein 1, which is involved in the initial stage of the inflammatory response, possibly through its critical roles as a tumor suppressor or promoter (40), was upregulated following 2-h borax treatment in the present study. Furthermore, prostaglandin-endoperoxide synthase 2, a principal inflammatory mediator and a UV-inducible enzyme the catalyzes the first step in the synthesis of prostaglandin E2 (41), was also upregulated. Additionally, TNFAIP3 and caspase--6, which are associated with inflammation and stress reaction (42), were also found to be upregulated. Notably, TNFAIP3 acts as a critical molecular switch to discriminate tumor necrosis factor-induced NF-κB signaling from the activated JNK signaling pathways in hepatocytes when stimulated with varying cytokine concentrations under normal or pathological conditions (43). These findings implicate downregulated/upregulated genes following borax treatment impact the migration and invasion of tumor cells, DNA binding signal transduction, inflammation and stress reactions. However, the specific mechanisms involved require further study.

The expression levels of 1,763 genes were changed in cells from the 24-h treatment group compared with those in the control group. Specifically, 719 genes were downregulated and 1,044 genes were upregulated (Fig. 1). Among them, the downregulated genes included B3GALT6, a critical enzyme catalyzing the formation of the tetrasaccharide linkage region, the mutation of which results in proteoglycan maturation defects (44). In the present study, FAM20B was downregulated in the 24-h treatment group. Notably, it was previously indicated that FAM20B deletion is associated with Ehlers-Danlos syndrome (45,46). UBE4B was also downregulated in cells from the 24-h treatment group in the present study. A previous study revealed that silencing of UBE4B expression inhibited the proliferation, colony formation, migration and invasion of liver cancer cells *in vitro*, and resulted in significant apoptosis. Therefore, it was suggested that this gene may be a good prognostic candidate for liver cancer (47). The overexpression of UBE4B, which is

Table IV. Differentially expressed genes involved in signal transduction (24 h vs. control group).

Pathway/ Genebank ID	Probe_Set_ID	Gene symbol	Description of expression product	Fold change	P-values	Regulation after borax treeatment
hsa04110:Cell cycle						
NM_002392	TC12000606.hg.1	MDM2	Mdm2, p53 E3 ubiquitin protein ligase homolog	13.8	0.00010	Up
NM_001199741	TC01000745.hg.1	GADD45A	Growth arrest and DNA-damage-inducible, alpha	7.9	0.00006	Up
NM_000389	TC06000532.hg.1	CDKN1A	Cyclin-dependent kinase inhibitor 1A (p21, Cip1)	4.4	0.00015	Up
NM_001259	TC07001603.hg.1	CDK6	Cyclin-dependent kinase 6	4.3	0.00013	Up
NM_001079846	TC16000823.hg.1	CREBBP	CREB binding protein (CREBBP)	3.0	0.00007	Up
NM_001799	TC05000301.hg.1	CDK7	Cyclin-dependent kinase 7	2.8	0.00039	Up
NM_007637	TC10001228.hg.1	ZNF84	Zinc finger protein 84	2.42	0.00063	Up
NM_001789	TC03001374.hg.1	CDC25A	Cell division cycle 25 homolog A	2.4	0.00041	Up
NM_002553	TC07001724.hg.1	ORC5	Origin recognition complex, subunit 5	2.3	0.00012	Up
BC012827	TC01000545.hg.1	CDC20	Cell division cycle 20 homolog	2.2	0.00364	Up
NM126792	TC05001184.hg.1	B3GALT6	Beta 1,3-galactosyltransferase polypeptide 6	-18.97	0.00000	Down
NM009917	TC06001313.hg.1	FAM20B	Family with sequence similarity 20, member B	-5.13	0.00002	Down
NM_001262	TC01000619.hg.1	CDKN2C	Cyclin-dependent kinase inhibitor 2C (p18, inhibits CDK4)	-4.8	0.00364	Down
NM_003318	TC06000761.hg.1	TTK	TTK protein kinase	-3.7	0.00008	Down
NM_001237	TC04001516.hg.1	CCNA2	Cyclin A2 (CCNA2)	-3.5	0.00007	Down
NM_004701	TC15000449.hg.1	CCNB2	Cyclin B2 (CCNB2)	-2.7	0.00011	Down
NM_005611	TC16000448.hg.1	RBL2	Retinoblastoma-like 2 (p130)	-2.6	0.00001	Down
NM_001178138	TC03001849.hg.1	TFDP2	Transcription factor Dp-2 (E2F dimerization partner 2)	-2.5	0.00001	Down
NM_001786	TC02001182.hg.1	CDK1	Cyclin-dependent kinase 1	-2.5	0.00163	Down
NM_002388	TC06001799.hg.1	MCM3	Minichromosome maintenance complex component 3	-2.5	0.00000	Down
NM_057749	TC08001438.hg.1	CCNE2	Cyclin E2 (CCNE2)	-2.4	0.00622	Down
NM_001042749	TC0X000606.hg.1	STAG2	Stromal antigen 2 (STAG2	-2.2	0.00017	Down
NM_005915	TC02002376.hg.1	MCM6	Minichromosome maintenance complex component 6	-2.1	0.00019	Down
NM_001136197	TC19000070.hg.1	FZR1	Fizzy/cell division cycle 20 related 1	-2.1	0.00348	Down
NM_022809	TC05001829.hg.1	CDC25C	Cell division cycle 25 homolog C	-2.1	0.00092	Down
hsa04115:p53 signaling pathway						
NM_002392	TC12000606.hg.1	MDM2	Mdm2, p53 E3 ubiquitin protein ligase homolog	13.8	0.00010	Up
NM_008870	TC13000386.hg.1	IER3	Immediate early response 3	8.47	0.00200	Up
NM_001199741	TC01000745.hg.1	GADD45A	Growth arrest and DNA-damage-inducible, alpha	7.9	0.00006	Up
NM_021127	TC18000213.hg.1	PMAIP1	Phorbol-12-myristate-13-acetate-induced protein 1	6.1	0.00001	Up
NM_000389	TC06000532.hg.1	CDKN1A	Cyclin-dependent kinase inhibitor 1A	4.4	0.00015	Up
NM_001259	TC07001603.hg.1	CDK6	Cyclin-dependent kinase 6	4.3	0.00013	Up
NM_001172477	TC08001496.hg.1	RRM2B	Ribonucleotide reductase M2 B	3.7	0.00015	Up
NM_001199933	TC06001997.hg.1	SESN1	Sestrin 1	3.6	0.00004	Up
NM_000602	TC07000643.hg.1	SERPINE1	serpin peptidase inhibitor, clade E (nexin, plasminogen activator inhibitor type 1), member 1	2.2	0.00406	Up

Table IV. Continued.

Pathway/ Genebank ID	Probe_Set_ID	Gene symbol	Description of expression product	Fold change	P-values	Regulation after borax treeatment
NM_004324	TC19000716.hg.1	BAX	BCL2-associated X protein	2.2	0.00672	Up
NM_001034	TC02000057.hg.1	RRM2	ribonucleotide reductase M2	-2.9	0.00010	Down
NM_002639	TC18000226.hg.1	SERPINB5	Serpin peptidase inhibitor, clade B (ovalbumin), member 5	-2.8	0.00756	Down
NM_001196	TC01000866.hg.1	BID	BH3 interacting domain death agonist	-2.5	0.00002	Down
NM_016426	TC22000394.hg.1	GTSE1	G-2 and S-phase expressed 1	-2.4	0.00019	Down
NM_003620	TC17000739.hg.1	PPM1D	Protein phosphatase, Mg2+/Mn2+ dependent, 1D	4.5	0.00005	Up
NM_003842	TC08001049.hg.1	TNFRSF10B	Tumor necrosis factor receptor superfamily, member 10b	3.8	0.00005	Up
NM_031459	TC01000377.hg.1	SESN2	Sestrin 2	3.7	0.00119	Up
NM_003246	TC15000270.hg.1	THBS1	Thrombospondin 1	2.5	0.00013	Up
NM_010277	TC66000070.hg.1	UBE4B	Ubiquitination factor E4B	-17.44	0.00000	Down
NM_005351	TC62000079.hg.1	PLOD1	Procollagen-lysine, 2-oxoglutarate 5-dioxygenase 1	-16.78	0.00104	Down
NM_004701	TC15000449.hg.1	CCNB2	Cyclin B2	-2.7	0.00011	Down
NM_001786	TC02001182.hg.1	CDK1	Cyclin-dependent kinase 1	-2.5	0.00163	Down
NM_057749	TC08001438.hg.1	CCNE2	Cyclin E2	-2.4	0.00622	Down
NM_022470	TC03002022.hg.1	ZMAT3	Zinc finger, matrin-type 3	-2.2	0.00161	Down
hsa04668:TNF signaling pathway						
NM_006290	TC06001027.hg.1	TNFAIP3	Tumor necrosis factor, alpha-induced protein 3	20.2	0.00007	Up
NM_006941	TC11001948.hg.1	TCF19	Transcription factor 19	8.96	0.00064	Up
NM_001168319	TC06000087.hg.1	EDN1	Endothelin 1	3.0	0.00025	Up
NM_001145138	TC11001939.hg.1	RELA	V-rel reticuloendotheliosis viral oncogene homolog A (avian)	3.0	0.00002	Up
NM_001244134	TC10002935.hg.1	MAP3K8	Mitogen-activated protein kinase kinase kinase 8	2.9	0.00013	Up
NM_000214	TC20000621.hg.1	JAG1	Jagged 1	2.7	0.00019	Up
NM_000963	TC01003638.hg.1	PTGS2	Prostaglandin-endoperoxide synthase 2 (prostaglandin G/H synthase and cyclooxygenase)	2.6	0.02677	Up
NM_001166	TC11000957.hg.1	BIRC2	Baculoviral IAP repeat containing 2	2.3	0.00069	Up
NM_000600	TC05001366.hg.1	IL6	Interleukin-6	2.2	0.00002	Up
NM_182810	TC22000317.hg.1	ATF4	Activating transcription factor 4 (tax-responsive enhancer element B67)	2.2	0.00548	Up
NM-029914	TC61000040.hg.1	UBIAD1	UbiA prenyltransferase domain containing 1	-16.88	0.00108	Down
NM_001256045	TC03001824.hg.1	PIK3CB	Phosphoinositide-3-kinase, catalytic, beta polypeptide	-4.7	0.00000	Down
NM_001065	TC12001135.hg.1	TNFRSF1A	Tumor necrosis factor receptor superfamily, member 1A	-4.0	0.00035	Down
NM_002758	TC17000807.hg.1	MAP2K6	Mitogen-activated protein kinase kinase 6	-4.0	0.00021	Down
NM_002982	TC17000383.hg.1	CCL2	Chemokine (C-C motif) ligand 2	-2.6	0.03428	Down
NM_001114172	TC01002616.hg.1	PIK3R3	Phosphoinositide-3-kinase, regulatory subunit 3 (gamma)	-2.3	0.00083	Down
NM_005027	TC19002628.hg.1	PIK3R2	Phosphoinositide-3-kinase, regulatory subunit 2 (beta)	-2.3	0.00044	Down

Table IV. Continued.

Pathway/ Genebank ID	Probe_Set_ID	Gene symbol	Description of expression product	Fold change	P-values	Regulation after borax treeatment
NM_001136153	TC06004121.hg.1	ATF6B	Activating transcription factor 6 beta	-2.1	0.00045	Down
NM_001199427	TC14000786.hg.1	TRAF3	TNF receptor-associated factor 3 (TRAF3)	-2.1	0.00073	Down
hsa04152:AMPK signaling pathway						
NM_003749	TC13000871.hg.1	IRS2	Insulin receptor substrate 2	3.5	0.00044	Up
NM_000875	TC15000949.hg.1	IGF1R	Insulin-like growth factor 1 receptor	3.5	0.00188	Up
NM_181715	TC01003280.hg.1	CRTC2	CREB regulated transcription coactivator 2	3.0	0.00176	Up
NM_006253	TC12000936.hg.1	PRKAB1	Protein kinase, AMP-activated, beta 1 non-catalytic subunit	2.7	0.00031	Up
NM_012238	TC10000400.hg.1	SIRT1	Sirtuin 1	2.5	0.00023	Up
NM_001018053	TC01001731.hg.1	PFKFB2	6-phosphofructo-2-kinase/ fructose-2,6-biphosphatase 2	2.4	0.00008	Up
NM_000859	TC05000363.hg.1	HMGCR	3-hydroxy-3-methylglutaryl-CoA reductase	-4.8	0.00001	Down
NM_001256045	TC03001824.hg.1	PIK3CB	Phosphoinositide-3-kinase, catalytic, beta polypeptide	-4.7	0.00000	Down
NM_005063	TC10000721.hg.1	SCD	Stearoyl-CoA desaturase (delta-9-desaturase)	-4.6	0.00323	Down
NM_001237	TC04001516.hg.1	CCNA2	Cyclin A2	-3.5	0.00007	Down
NM_001199756	TC01001771.hg.1	PPP2R5A	Protein phosphatase 2, regulatory subunit B', alpha	-2.8	0.00000	Down
NM_004104	TC17001973.hg.1	FASN	Fatty acid synthase	-2.6	0.00024	Down
NM_198834	TC17001406.hg.1	ACACA	Acetyl-CoA carboxylase alpha	-2.6	0.00073	Down
NM_005027	TC19002628.hg.1	PIK3R2	Phosphoinositide-3-kinase, regulatory subunit 2	-2.3	0.00044	Down
NM_001114172	TC01002616.hg.1	PIK3R3	Phosphoinositide-3-kinase, regulatory subunit 3 (gamma)	-2.3	0.00083	Down
NM_005037	TC03000069.hg.1	PPARG	Peroxisome proliferator-activated receptor gamma	-2.1	0.00108	Down
NM_001177562	TC11002284.hg.1	PPP2R1B	Protein phosphatase 2, regulatory subunit A	-2.0	0.01473	Down
hsa04621:NOD-like receptor signaling pathway						
NM_006290	TC06001027.hg.1	TNFAIP3	Tumor necrosis factor, alpha-induced protein 3	20.2	0.00007	Up
NM_001562	TC11002293.hg.1	IL18	Interleukin-18	3.1	0.00033	Up
NM_001145138	TC11001939.hg.1	RELA	V-rel reticuloendotheliosis viral oncogene homolog A	3.0	0.00002	Up
NM_001166	TC11000957.hg.1	BIRC2	Baculoviral IAP repeat containing 2	2.3	0.00069	Up
NM_004620	TC11001560.hg.1	TRAF6	TNF receptor-associated factor 6, E3 ubiquitin protein ligase	2.3	0.00000	Up
NM_000600	TC05001366.hg.1	IL6	Interleukin-6	2.2	0.00002	Up
NM_001006600	TC05000280.hg.1	ERBB2IP	Erbb2 interacting protein	-3.1	0.00030	Down
NM_002982	TC17000383.hg.1	CCL2	Chemokine (C-C motif) ligand 2	-2.6	0.03428	Down
NM_001017963	TC14001526.hg.1	HSP90AA1	Heat shock protein 90 kDa alpha (cytosolic), class A member 1	-2.5	0.00029	Down

widely accepted as a p53 upstream target gene, contributes to the migration and invasion of tumor cells (48,49). UBIAD1, also known as UbiA prenyltransferase domain-containing protein 1, functions as an important regulator in the cell progression of bladder and prostate cancer, as well as vascular integrity, possibly through its modulation of metabolism of intracellular

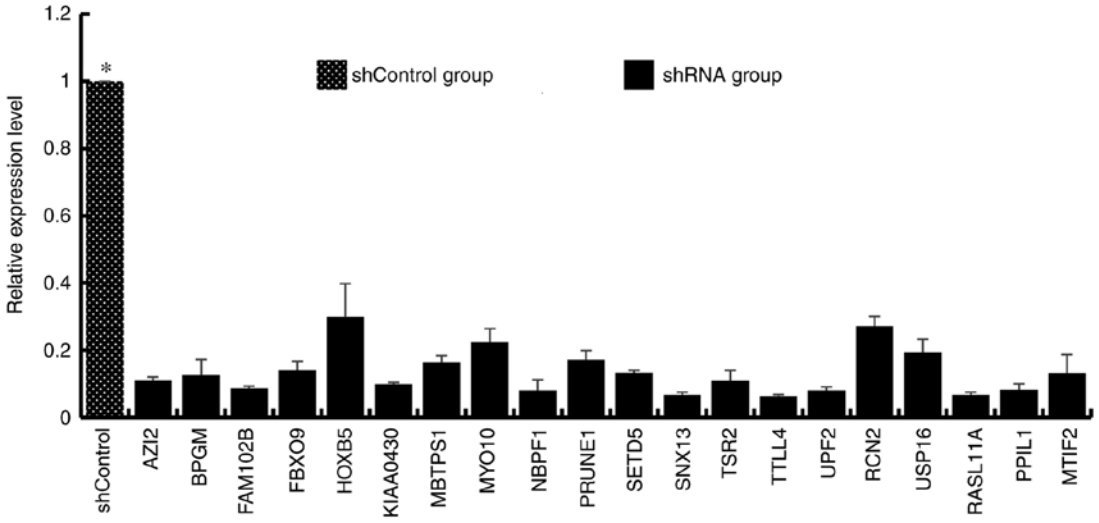

Figure 5. The decreased expression of genes was established following transfection with each shRNA with real-time PCR. *P<0.05, vs. shControl. shRNA, short hairpin RNA.

cholesterol and protection against oxidative stress (50). UBIAD1 was also downregulated. Additionally, PLOD1, which is associated with cell apoptosis, cell cycle and metastasis (51), was also found to be downregulated.

In the present study, 24-h treatment with borax upregulated the expression of several genes, including ZNF84, which is also known as a zinc finger transcription factor gene (52). ZNF84 is located in chromosome 12q24.33, which is correlated with recurrent breakpoints and allelic loss in a few types of cancer (52,53). Immediate early response 3 was another upregulated gene that normally regulates apoptosis, proliferation and the maintenance of HCCs (54,55). TCF19, which was also upregulated, has been identified to be a good prognostic candidate for HCC, thereby becoming a promising candidate for preclinical and/or clinical studies to determine its potential risk in HCCs (56).

Distinct sets of genes were found to be altered after different treatment durations, namely, borax treatments for either 2 or 24 h in HepG2 cells. Exposure to borax for 2 h altered the expression levels of genes encoding proteins involved in signal transduction underlying stress response, biopolymer metabolic process, the inflammatory response (e.g., NF-κB and caspase--6) and unfolded protein response among other possibilities. Notably, the results for cells from the 2-h treatment group revealed the disruption of certain metabolic processes involved in inflammation and stress response. Accordingly, borax treatment for 24 h caused the dysregulation of genes involved in a number of signaling pathways, which are associated with enhanced cell proliferation and apoptosis underlying the disruption of both vascular integrity and suppression of tumor cell progression (16), indicating that the disruption of those signaling pathways may contribute to carcinogenesis in borax-treated HepG2 cells.

Enriched GO analyses in the present study revealed that the significantly enriched gene sets included the response to primary metabolic process, response to stimulus, biosynthetic process, developmental process, apoptotic process, immune system process, binding, catalytic activity, cell part, organelles, and others. In the present study, the downregulation of PRUNE1, NBPF1, PPcaspase-1, UPF2, and MBTPS1 suggested that they inhibited the growth of HepG2 cells. For instance, PRUNE1 is a member of the Asp-His-His phosphoesterase protein superfamily, which is involved in cell motility and is implicated in cancer progression (57). NBPF1 is a tumor suppressor in several cancer types and can act as a tumor suppressor modulating cell apoptosis, possibly through the inhibition of various proteins involved in the cell cycle (58). NBPF1 is also implicated in cancer progression (59). PPcaspase-1 has also been reported to be upregulated in human colon cancer cells. Accordingly, small interfering RNA-mediated PPcaspase-1 knockdown resulted in cell apoptosis in those cells (60). Therefore, precise modulations of the expression level of these critical genes leads to accurate regulation of cellular activity, thereby contributing to the suppressed initiation of cancer progression. Notably, future progress in identifying the basic features of these essential proteins may provide further insights into the diagnosis and prognosis of certain types of human cancer and may also aid the production of novel strategies to develop more effective and efficient therapeutic agents against those types of cancer.

To conclude, 2- and 24-h borax treatment caused significant alterations in the expression levels of various genes. However, based on the length of treatment different sets of genes were altered. Dysregulated genes were identified to be involved in various critical signaling pathways underlying biological processes, including the inflammatory response, stress response, cell apoptosis, signal transduction and cell-to-cell signaling. Some of these changes in those biological processes persisted 24 h after treatment. Thus, it was demonstrated that borax could induce significant alterations in gene expression. However, further studies are required to determine whether these changes are ascribed to genetic alterations in the promoter or regulatory regions of dysregulated genes. Notably, these studies could bring further insights into how borax affects gene expression. The present study provides the fundamental basis for exploring the carcinogenicity of borax treatment in HepG2 to reveal the underlying cellular and molecular mechanisms, the basic

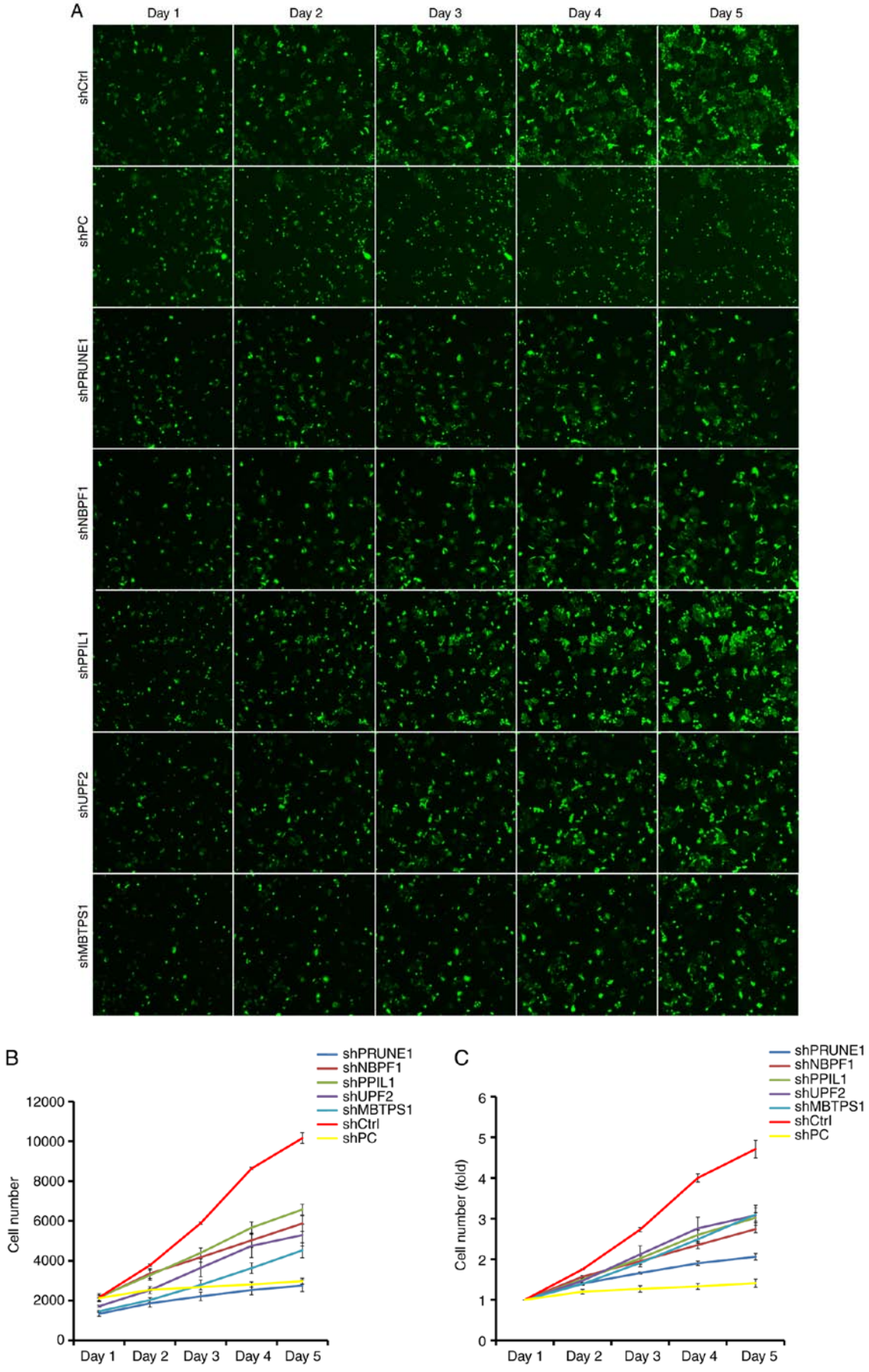

Figure 6. HepG2 cells were transfected with RNAiMax and counts of live adherent HepG2 in cell culture using a Celigo cytometer at the time points indicated. (A) GFP expression of cells infected with different AdGFP-iRNA. (B) Graphs indicated the number of viable cells. (C) Graphs indicated cell growth according to fold change [fold change=shControl/experimental group (transfected with RNAiMax) ≥1.5, P<0.05]. Ctrl, non-targeting shRNA, PC, positive control (specific-targeting shRNA); AdGFP, adenoviral green fluorescent protein.

biological characteristics and associated pathways, which warrant further investigation.

Acknowledgements

Not applicable.

Funding

This work was funded by the National Natural Scientific Foundation of China (grant no. 81872509), the Natural Science Foundation of Hubei Provincial Department of Education (grant no. D20172101), the Hubei Provincial Technology Innovation Project (grant no. 2017ACA176), the Hubei Province Health and Family Planning Scientific Research Project (grant no. WJ2019M054), the Natural Science Foundation of Hubei Provincial Department of Education (grant no. Q20162113) and the Natural Science Foundation of the Bureau of Science and Technology of Shiyan City (grant no. 18Y76, 17Y47).

Availability of data and materials

The datasets used and/or analyzed during the current study are available from the corresponding author on reasonable request.

Authors' contributions

LW, YW, ZGT and YSZ conceived and designed the experiments. LW, ZPZ, JZ, HMW, GMW and SW contributed reagents, materials and analysis tools and performed the experiments. LW, WBZ, QHC, LHY and MXL analyzed and interpreted the experimental data. LW was a major contributor in writing the manuscript. All authors read and approved the final manuscript.

Ethics approval and consent to participate

Not applicable.

Patient consent for publication

Not applicable.

Competing interests

The authors declare that they have no competing interests.

References

1. Routray I and Ali S: Boron induces lymphocyte proliferation and modulates the priming effects of lipopolysaccharide on macrophages. PLoS One 11: e0150607, 2016.
2. Neiner D, Sevryugina YV, Harrower LS and Schubert DM: Structure and properties of sodium enneaborate, $Na_2[B_8O_{11}(OH)_4]\cdot B(OH)_3\cdot 2H_2O$. Inorg Chem 56: 7175-7181, 2017.
3. Alak G, Parlak V, Yeltekin AÇ, Ucar A, Çomaklı S, Topal A, Atamanalp M, Özkaraca M and Türkez H: The protective effect exerted by dietary borax on toxicity metabolism in rainbow trout (*Oncorhynchus mykiss*) tissues. Comp Biochem Physiol C Toxicol Pharmacol 216: 82-92, 2019.
4. Alak G, Parlak V, Aslan ME, Ucar A, Atamanalp M and Turkez H: Borax supplementation alleviates hematotoxicity and DNA damage in rainbow trout (*Oncorhynchus mykiss*) exposed to copper. Biol Trace Elem Res 187: 536-542: 2019.
5. Hussain SA, Abood SJ and Gorial FI: The adjuvant use of calcium fructoborate and borax with etanercept in patients with rheumatoid arthritis: Pilot study. J Intercult Ethnopharmacol 6: 58-64, 2016.
6. Ince S, Kucukkurt I, Cigerci IH, Fatih Fidan A and Eryavuz A: The effects of dietary boric acid and borax supplementation on lipid peroxidation, antioxidant activity, and DNA damage in rats. J Trace Elem Med Biol 24: 161-164, 2010.
7. Sandeep Varma R, Shamsia S, Thiyagarajan OS, Vidyashankar S and Patki PS: Yashada bhasma (Zinc calx) and Tankana (Borax) inhibit Propionibacterium acne and suppresses acne induced inflammation in vitro. Int J Cosmet Sci 36: 361-368, 2014.
8. López-Cabrera Y, Castillo-García EL, Altamirano-Espino JA, Pérez-Capistran T, Farfán-García ED, Trujillo-Ferrara JG and Soriano-Ursúa MA: Profile of three boron-containing compounds on the body weight, metabolism and inflammatory markers of diabetic rats. J Trace Elem Med Biol 50: 424-429, 2018.
9. Geyikoglu F and Turkez H: Boron compounds reduce vanadium tetraoxide genotoxicity in human lymphocytes. Environ Toxicol Pharmacol 26: 342-347, 2008.
10. Gülsoy N, Yavas C and Mutlu Ö: Genotoxic effects of boric acid and borax in zebrafish, Danio rerio using alkaline comet assay. EXCLI J 14: 890-899, 2015.
11. Sarkar PK, Prajapati PK, Shukla VJ and Ravishankar B: Evaluation of processed borax as antidote for aconite poisoning. J Ethnopharmacol 205: 138-146, 2017.
12. Capkin E, Ozcelep T, Kayis S and Altinok I: Antimicrobial agents, triclosan, chloroxylenol, methylisothiazolinone and borax, used in cleaning had genotoxic and histopathologic effects on rainbow trout. Chemosphere 182: 720-729, 2017.
13. Pongsavee M: Genotoxic effects of borax on cultured lymphocytes. Southeast Asian J Trop Med Public Health 40: 411-418, 2009.
14. Pongsavee M: Effect of borax on immune cell proliferation and sister chromatid exchange in human chromosomes. J Occup Med Toxicol 4: 27, 2009.
15. Çelikezen FÇ, Toğar B, Özgeriş FB, İzgi MS and Türkez H: Cytogenetic and oxidative alterations after exposure of cultured human whole blood cells to lithium metaborate dehydrate. Cytotechnology 68: 821-827, 2016.
16. Wei Y, Yuan FJ, Zhou WB, Wu L, Chen L, Wang JJ and Zhang YS: Borax-induced apoptosis in HepG2 cells involves p53, Bcl-2, and Bax. Genet Mol Res 15, 2016.
17. Brocato J and Costa M: Basic mechanics of DNA methylation and the unique landscape of the DNA methylome in metal-induced carcinogenesis. Crit Rev Toxicol 43: 493-514, 2013.
18. Hazman Ö, Bozkurt MF, Fidan AF, Uysal FE and Çelik S: the effect of boric acid and borax on oxidative stress, inflammation, ER stress and apoptosis in cisplatin toxication and nephrotoxicity developing as a result of toxication. Inflammation 41: 1032-1048, 2018.
19. Oh SH and Lim SC: A rapid and transient ROS generation by cadmium triggers apoptosis via caspase-dependent pathway in HepG2 cells and this is inhibited through N-acetylcysteine-mediated catalase upregulation. Toxicol Appl Pharmacol 212: 212-223, 2006.
20. Cartularo L, Laulicht F, Sun H, Kluz T, Freedman JH and Costa M: Gene expression and pathway analysis of human hepatocellular carcinoma cells treated with cadmium. Toxicol Appl Pharmacol 288: 399-408, 2015.
21. Livak KJ and Schmittgen TD: Analysis of relative gene expression data using real-time quantitative PCR and the 2(-Delta Delta C(T)) method. Methods 25: 402-408, 2001.
22. Zhang DY, Liu Z, Lu Z, Sun WL, Ma X, Zhang P, Wu BQ and Cui PY: Lentivirus-mediated overexpression of HSDL2 suppresses cell proliferation and induces apoptosis in cholangiocarcinoma. Onco Targets Ther 11: 7133-7142, 2018.
23. Zheng J, You W, Zheng C, Wan P, Chen J, Jiang X, Zhu Z, Zhang Z, Gong A, Li W, *et al*: Knockdown of FBXO39 inhibits proliferation and promotes apoptosis of human osteosarcoma U-2OS cells. Oncol Lett 16: 1849-1854, 2018.
24. Yamada KE and Eckhert CD: Boric acid activation of eIF2α and Nrf2 Is PERK dependent: A mechanism that explains how boron prevents DNA damage and enhances antioxidant status. Biol Trace Elem Res 188: 2-10, 2019.
25. Matencio A, Navarro-Orcajada S, García-Carmona F and López-Nicolás JM: Ellagic acid-borax fluorescence interaction: Application for novel cyclodextrin-borax nanosensors for analyzing ellagic acid in food samples. Food Funct 9: 3683-3687, 2018.

26. Donoiu I, Militaru C, Obleagă O, Hunter JM, Neamţu J, Biţă A, Scorei IR and Rogoveanu OC: Effects of boron-containing compounds on cardiovascular disease risk factors-a review. J Trace Elem Med Biol 50: 47-56, 2018.
27. Worm DJ, Els-Heindl S, Kellert M, Kuhnert R, Saretz S, Koebberling J, Riedl B, Hey-Hawkins E and Beck-Sickinger AG: A stable meta-carborane enables the generation of boron-rich peptide agonists targeting the ghrelin receptor. J Pept Sci 24: e3119, 2018.
28. Rico P, Rodrigo-Navarro A and Salmerón-Sánchez M: Borax-Loaded PLLA for promotion of myogenic differentiation. Tissue Eng Part A 21: 2662-2672, 2015.
29. Das BC, Thapa P, Karki R, Schinke C, Das S, Kambhampati S, Banerjee SK, Van Veldhuizen P, Verma A, Weiss LM and Evans T: Boron chemicals in diagnosis and therapeutics. Future Med Chem 5: 653-676, 2013.
30. Turkez H: Effects of boric acid and borax on titanium dioxide genotoxicity. J Appl Toxicol 28: 658-664, 2008.
31. Jensen JP: The rise and fall of borax as an antiepileptic drug. Arch Neurol 63: 621-622, 2006.
32. Meyer-Hamme G, Beckmann K, Radtke J, Efferth T, Greten HJ, Rostock M and Schröder S: A survey of chinese medicinal herbal treatment for chemotherapy-induced oral mucositis. Evid Based Complement Alternat Med 2013: 284959, 2013.
33. Landolph JR: Cytotoxicity and negligible genotoxicity of borax and borax ores to cultured mammalian cells. Am J Ind Med 7: 31-43, 1985.
34. Chen CP, Sun ZL, Lu X, Wu WX, Guo WL, Lu JJ, Han C, Huang JQ and Fang Y: MiR-340 suppresses cell migration and invasion by targeting MYO10 in breast cancer. Oncol Rep 35: 709-716, 2016.
35. Makowska KA, Hughes RE, White KJ, Wells CM and Peckham M: Specific myosins control actin organization, cell morphology, and migration in prostate cancer cells. Cell Rep 13: 2118-2125, 2015.
36. Zhang H, He P, Huang R, Sun L, Liu S, Zhou J, Guo Y, Yang D and Xie P: Identification and bioinformatic analysis of dysregulated microRNAs in human oligodendroglial cells infected with borna disease virus. Mol Med Rep 14: 4715-4722, 2016.
37. Pinto JA, Rolfo C, Raez LE, Prado A, Araujo JM, Bravo L, Fajardo W, Morante ZD, Aguilar A, Neciosup SP, *et al*: In silico evaluation of DNA Damage Inducible Transcript 4 gene (DDIT4) as prognostic biomarker in several malignancies. Sci Rep 7: 1526, 2017.
38. Shatov VM, Weeks SD, Strelkov SV and Gusev NB: The role of the arginine in the conserved N-terminal domain RLFDQxFG motif of human small heat shock proteins HspB1, HspB4, HspB5, HspB6, and HspB8. Int J Mol Sci 19: pii: E2112, 2018.
39. Konda JD, Olivero M, Musiani D, Lamba S and Di Renzo MF: Heat-shock protein 27 (HSP27, HSPB1) is synthetic lethal to cells with oncogenic activation of MET, EGFR and BRAF. Mol Oncol 11: 599-611, 2017.
40. Mohamad T, Kazim N, Adhikari A and Davie JK: EGR1 interacts with TBX2 and functions as a tumor suppressor in rhabdomyosarcoma. Oncotarget 9: 18084-18098, 2018.
41. Li H, Wang J, Liu X and Cheng Q: MicroRNA-204-5p suppresses caspase-6-mediated inflammatory response and chemokine generation in HK-2 renal tubular epithelial cells by targeting caspase-6R. Biochem Cell Biol 97: 109-117, 2019.
42. Zhai Y, Lin P, Feng Z, Lu H, Han Q, Chen J, Zhang Y, He Q, Nan G, Luo X, *et al*: TNFAIP3-DEPTOR complex regulates inflammasome secretion through autophagy in ankylosing spondylitis monocytes. Autophagy 14: 1629-1643, 2018.
43. Pinna F, Bissinger M, Beuke K, Huber N, Longerich T, Kummer U, Schirmacher P, Sahle S and Breuhahn K: A20/TNFAIP3 discriminates tumor necrosis factor (TNF)-Induced NF-κB from JNK pathway activation in hepatocytes. Front Physiol 8: 610, 2017.
44. Wen J, Xiao J, Rahdar M, Choudhury BP, Cui J, Taylor GS, Esko JD and Dixon JE: Xylose phosphorylation functions as a molecular switch to regulate proteoglycan biosynthesis. Proc Natl Acad Sci USA 111: 15723-15728, 2014.
45. Taylan F and Mäkitie O: Abnormal proteoglycan synthesis due to gene defects causes skeletal diseases with overlapping phenotypes. Horm Metab Res 48: 745-754, 2016.
46. Van Damme T, Pang X, Guillemyn B, Gulberti S, Syx D, De Rycke R, Kaye O, de Die-Smulders CEM, Pfundt R, Kariminejad A, *et al*: Biallelic B3GALT6 mutations cause spondylodysplastic Ehlers-Danlos syndrome. Hum Mol Genet 27: 3475-3487, 2018.
47. Zhang XF, Pan QZ, Pan K, Weng DS, Wang QJ, Zhao JJ, He J, Liu Q, Wang DD, Jiang SS, *et al*: Expression and prognostic role of ubiquitination factor E4B in primary hepatocellular carcinoma. Mol Carcinog 55: 64-76, 2016.
48. Periz G, Lu J, Zhang T, Kankel MW, Jablonski AM, Kalb R, McCampbell A and Wang J: Regulation of protein quality control by UBE4B and LSD1 through p53-mediated transcription. PLoS Biol 13: e1002114, 2015.
49. Wang B, Wu H, Chai C, Lewis J, Pichiorri F, Eisenstat DD, Pomeroy SL and Leng RP: MicroRNA-1301 suppresses tumor cell migration and invasion by targeting the p53/UBE4B pathway in multiple human cancer cells. Cancer Lett 401: 20-32, 2017.
50. Okano T: A new horizon in vitamin K research. Yakugaku Zasshi 136: 1141-1159, 2016 (In Japanese).
51. Li L, Wang W, Li X and Gao T: Association of ECRG4 with PLK1, CDK4, PLOD1 and PLOD2 in esophageal squamous cell carcinoma. Am J Transl Res 9: 3741-3748, 2017.
52. Rosati M, Rocchi M, Storlazzi CT and Grimaldi G: Assignment to chromosome 12q24.33, gene organization and splicing of the human KRAB/FPB containing zinc finger gene ZNF84. Cytogenet Cell Genet 94: 127-130, 2001.
53. Assou S, Cerecedo D, Tondeur S, Pantesco V, Hovatta O, Klein B, Hamamah S and De Vos J: A gene expression signature shared by human mature oocytes and embryonic stem cells. BMC Genomics 10: 10, 2009.
54. Zhou Q, Hahn JK, Neupane B, Aidery P, Labeit S, Gawaz M and Gramlich M: Dysregulated ier3 expression is associated with enhanced apoptosis in titin-based dilated cardiomyopathy. Int J Mol Sci 18: pii: E723, 2017.
55. Tran DDH, Koch A, Allister A, Saran S, Ewald F, Koch M, Nashan B and Tamura T: Treatment with MAPKAP2 (MK2) inhibitor and DNA methylation inhibitor, 5-aza dC, synergistically triggers apoptosis in hepatocellular carcinoma (HCC) via tristetraprolin (TTP). Cell Signal 28: 1872-1880, 2016.
56. Mathew S, Abdel-Hafiz H, Raza A, Fatima K and Qadri I: Host nucleotide polymorphism in hepatitis B virus-associated hepatocellular carcinoma. World J Hepatol 8: 485-498, 2016.
57. Zollo M, Ahmed M, Ferrucci V, Salpietro V, Asadzadeh F, Carotenuto M, Maroofian R, Al-Amri A, Singh R, Scognamiglio I, *et al*: PRUNE is crucial for normal brain development and mutated in microcephaly with neurodevelopmental impairment. Brain 140: 940-952, 2017.
58. Li D, Li P, Wu J, Yi J, Dou Y, Guo X, Yin Y, Wang D, Ma C and Qiu L: Methylation of NBPF1 as a novel marker for the detection of plasma cell-free DNA of breast cancer patients. Clin Chim Acta 484: 81-86, 2018.
59. Andries V, Vandepoele K, Staes K, Berx G, Bogaert P, Van Isterdael G, Ginneberge D, Parthoens E, Vandenbussche J, Gevaert K and van Roy F: NBPF1, a tumor suppressor candidate in neuroblastoma, exerts growth inhibitory effects by inducing a G1 cell cycle arrest. BMC Cancer 15: 391, 2015.
60. Stegmann CM, Lührmann R and Wahl MC: The crystal structure of PPcaspase-1 bound to cyclosporine A suggests a binding mode for a linear epitope of the SKIP protein. PLoS One 5: e10013, 2010.